УДК 539.17.01

CLUSTER AND SINGLE-PARTICLE DISTRIBUTIONS IN NUCLEUS-NUCLEUS INTERACTIONS

B.A.Kulakov, J.Karachuk

Relativistic nuclear reactions, π^- – C (p_{beam} = 40 GeV/c), Mg – Mg (p_{beam} = 4.5 A GeV/c), and C – C (p_{beam} = 4.2 A GeV/c), are compared by using Lorentz-invariant variables b_{ik}. These variables are used to compare and classify nuclear reactions of various types in a wide range of energies. Different algorithms of clusters separation in the four-velocity space are compared. Experimental distributions are analysed by means of invariant variables in the space to understand the difference of behaviour of particles and clusters for these reactions. Universal properties of hadron clusters are presented.

The investigation has been performed at the Laboratory of High Energies, JINR.

Кластерные и одночастичные распределения в ядро-ядерных взаимодействиях

Б.А.Кулаков, Ю.Карачук

Проведено сравнение релятивистских ядерных реакций π^- – C ($p_{пучок}$ = 40 ГэВ/с), Mg – Mg ($p_{пучок}$ = 4,5 A ГэВ/с) и C – C ($p_{пучок}$ = 4,2 A ГэВ/с) с помощью лоренц-инвариантных переменных b_{ik}. Эти переменные используются для сравнения и классификации ядерных реакций различных типов в широком диапазоне энергий. Проведено сравнение разных алгоритмов разделения кластеров в пространстве четырехмерных скоростей. Экспериментальные распределения были проанализированы с помощью инвариантных переменных в этом пространстве для выяснения разницы в поведении частиц и кластеров в этих реакциях. Представлены универсальные свойства адронных кластеров.

Работа выполнена в Лаборатории высоких энергий ОИЯИ.

1. Introduction

In [1—2] various hadron-hadron and hadron-nucleus reactions were analysed and it was proved that some properties of the hadron clusters do not depend either on the colliding objects, or on the incident momentum. In this paper we try to extend these investigations to nucleus-nucleus interactions at $p_{inc} \simeq 4$ momentum.

The method used in this article is based on the possibility of describing any nuclear reaction in the four-velocity space [1—2].

Every particle i is characterized by the vector

$$\hat{u}_i = (u_i^0, u_i^x, u_i^y, u_i^z) = \frac{\hat{p}_i}{m_i} = \left(\frac{E_i}{m_i}, \frac{p_i^x}{m_i}, \frac{p_i^y}{m_i}, \frac{p_i^z}{m_i} \right) \quad (1)$$

which indicates its position in this space. As $E_i^2 - \mathbf{p}_i^2 = m_i^2$, we have $\hat{u}_i^2 = 1$. The distance between two points in this space is called a relative invariant velocity and is defined as follows

$$b_{ik} = -(\hat{u}_i - \hat{u}_k)^2 = 2(\hat{u}_i \hat{u}_k - 1). \quad (2)$$

These Lorentz-invariant variables can be used to classify the nuclear processes [1—2]:

- For $b_{ik} << 1$ the hadrons can be treated as quasi-particles of nuclear matter;
- For $b_{ik} \sim 1$ the hadrons lose their individuality and the quark degrees of freedom become important;
- For $b_{ik} >> 1$ the hadrons should be considered as quark-gluon systems.

The invariant variables in the four-velocity space can be used to formulate in a simple way such general laws as the correlation depletion principle [4] as well as to separate hadron clusters by means of algorithms independent of the reference frame [1—3,5].

In this paper we shall use the single particles and clusters invariant distributions to analyse different nuclear reactions:

- π^- – C at $p_{beam} = 40$ GeV/c; 8791 events were registered in the propane bubble chamber; both positive and negative pions were measured [8];
- C – C at $p_{beam} = 4.2$ A GeV/c; 21439 events were obtained in the propane bubble chamber; π^+ and π^- mesons were measured [6];
- Mg – Mg at $p_{beam} = 4.5$ A GeV/c; 14218 central interactions were registered in the streamer chamber; only π^- mesons were measured [7].

Pion clusters in π^- – C at $p_{beam} = 40$ GeV/c were investigated in [1—2,8]. It was shown that for this reaction the asymptotic regime corresponding to large b_{ik} values and clear separation of clusters is reached. In this paper we shall compare those results with the ones obtained for Mg – Mg and C – C reactions at $p_{beam} \sim 4$ A GeV/c. These reactions correspond to the intermediate region $b_{ik} \sim 1$. This is why we think the comparative analysis would be very interesting.

2. Single Particle Distributions

We define the scalars X_i^B and X_i^T, which represent the part of the beam and target four-momenta carried by the secondary particle i.

As in [1—2] we estimate them:

$$X_i^B = \frac{\hat{p}_i \hat{p}_T}{\hat{p}_B \hat{p}_T} = \frac{m_i \hat{u}_i \hat{u}_T}{m_B \hat{u}_B \hat{u}_T}, \tag{3}$$

$$X_i^T = \frac{\hat{p}_i \hat{p}_B}{\hat{p}_B \hat{p}_T} = \frac{m_i \hat{u}_i \hat{u}_B}{m_T \hat{u}_B \hat{u}_T}, \tag{4}$$

where $\hat{p}_B(\hat{u}_B)$, $\hat{p}_T(\hat{u}_T)$ are the four-momenta (four-velocities) of the beam and the target.

These variables enable us to separate the fragmentation regions of the colliding objects.

In Figures 2a, 2b and 2c we present $XB - XT$ ($X_i^B - X_i^T$) plots for pions in the reactions Mg – Mg, C – C and π^- – C.

As one can see, for nucleus-nucleus collisions, the picture is similar irrespective of the mass number A. For both Mg – Mg and C – C reactions the particles cannot be found close to the axes, and the empty region gets larger when the X_i^B and X_i^T values grow.

It is also seen that the difference between these ones and the π^--nucleus reaction is significant. In this case the pions are close to the axes and remain close when the X_i^B and X_i^T values grow.

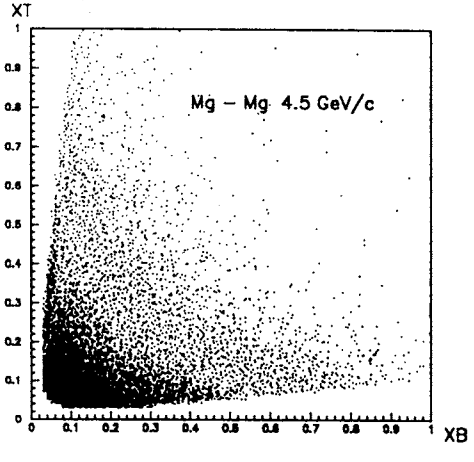

Fig.2a

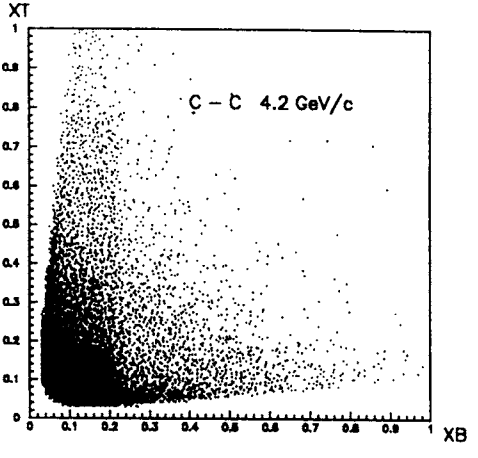

Fig.2b

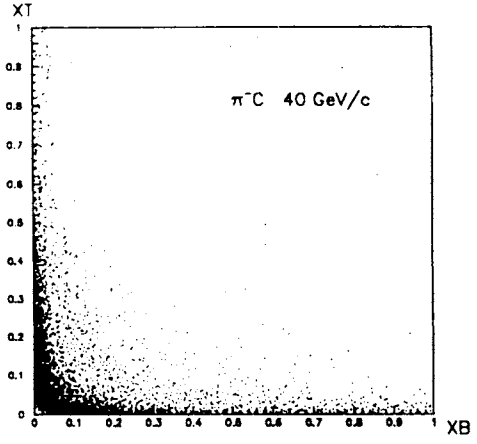

Fig.2c

We cannot say whether this happens due to the difference of incident impulses or because of different projectiles.

It is interesting to compare the pion distributions around the primary objects for different reactions. The distances from the pion i to the target and to the beam are

$$b_i^T = -(\hat{u}_i - \hat{u}_T)^2 = 2(\hat{u}_i \cdot \hat{u}_T - 1), \tag{5}$$

$$b_i^B = -(\hat{u}_i - \hat{u}_B)^2 = 2(\hat{u}_i \cdot \hat{u}_B - 1). \tag{6}$$

The invariant cross section $E_i \frac{d^3\sigma}{d\mathbf{p}_i}$ can be expressed as a function of these variables [1—2]. If we integrate over the solid angle, we obtain the following functions

$$F(b_i^T) = \frac{1}{\sigma} \int_\Omega \frac{2}{m_i^2} \frac{1}{\sqrt{\frac{(b_i^T)^2}{4} + b_i^T}} \frac{d\sigma d\Omega_i}{db_i^T d\Omega_i} \tag{7}$$

for the particles belonging to the target fragmentation region and

$$F(b_i^B) = \frac{1}{\sigma} \int_\Omega \frac{2}{m_i^2} \frac{1}{\sqrt{\frac{(b_i^B)^2}{4} + b_i^B}} \frac{d\sigma d\Omega_i}{db_i^B d\Omega_i} \tag{8}$$

for the beam region.

Table 2a

Reaction	Fit parameters	Target fragmentation	Beam fragmentation
Mg — Mg at 4.5 GeV/c	A_1	0.13 ± 0.01	0.13 ± 0.01
	t_1	2.67 ± 0.05	2.51 ± 0.04
	A_2	0.82 ± 0.03	0.75 ± 0.02
	t_2	1.15 ± 0.03	1.12 ± 0.03

Table 2b

Reaction	Fit parameters	Target fragmentation	Beam fragmentation
C — C at 4.2 GeV/c	A_1	0.32 ± 0.03	0.08 ± 0.02
	t_1	2.18 ± 0.04	2.50 ± 0.09
	A_2	0.28 ± 0.03	0.60 ± 0.02
	t_2	1.07 ± 0.09	1.36 ± 0.03

Table 2c

Reaction	Fit parameters	Target fragmentation	Beam fragmentation
$\pi^- C$ at 40 GeV/c	A_1	0.010 ± 0.001	0.005 ± 0.002
	t_1	11.1 ± 0.3	56 ± 4
	A_2	0.145 ± 0.005	0.021 ± 0.001
	t_2	4.7 ± 0.1	27 ± 2
	A_3	0.24 ± 0.02	0.037 ± 0.004
	t_3	1.02 ± 0.09	5.0 ± 0.6

These functions can be described as a sum of exponentials

$$F(x) = A_1 e^{\frac{-x}{t_1}} + A_2 e^{\frac{-x}{t_2}} + A_3 e^{\frac{-x}{t_3}}. \tag{9}$$

Tables 2a, 2b and 2c show the values obtained for the A_i and t_i coefficients as results of fitting.

These results show again the similarity between the Mg – Mg and C – C nucleus-nucleus reactions. For the π^- – C reaction the coefficients are different from the nucleus-nucleus ones and in this case we can also see the difference between the fragmentation regions of the incident π^- and of the target.

3. Clusters in the Four-Velocity Space

According to [1—3,5], a group of secondary particles, close to one another in this space, will be called a cluster. The cluster α contains n_α particles characterized by their four-velocities $\hat{u}_{i_\alpha}$. The cluster axis $\hat{V}_\alpha$ is

$$\hat{V}_\alpha = \frac{\sum_{i_\alpha=1}^{n_\alpha} \hat{u}_{i_\alpha}}{\sqrt{\left(\sum_{i_\alpha=1}^{n_\alpha} \hat{u}_{i_\alpha}\right)^2}}. \tag{10}$$

We can write the distance between a cluster particle and its axis as follows

$$b_{\alpha k_\alpha} = -(\hat{V}_\alpha - \hat{u}_{k_\alpha})^2. \tag{11}$$

The cluster width is represented by the mean value of this variable. The distance between clusters is written as

$$b_{\alpha\beta} = -(\hat{V}_\alpha - \hat{V}_\beta)^2. \tag{12}$$

The clusters are clearly separated if the distance between them is larger than the sum of their widths.

The first algorithm to create clusters used in this paper was proposed in [1—2].

This algorithm can be applyed if the number of secondary pions $n_{\pi^\pm} \geq 4$.

All the n secondary particles are supposed to belong either to the beam or to the target fragmentation regions, so they can be divided into two clusters: α and β, which contain n_α and n_β particles respectively ($n_\alpha + n_\beta = n$). From all the possible ways to divide these particles one has chosen the variant leading to the minimization of the following functional

$$A_2^n = \min\left[-\sum_{i_\alpha=1}^{n_\alpha} (\hat{V}_\alpha - \hat{u}_{i_\alpha})^2 - \sum_{i_\beta=1}^{n_\beta} (\hat{V}_\beta - \hat{u}_{i_\beta})^2\right]. \tag{13}$$

We shall take into consideration only those events which satisfy the conditions $b_{\alpha\beta} > b_{\min}$, where $b_{\min}$ is given and means the smallest value for the distance between the clusters which are considered still clearly separated. For π^- – C at 40 GeV/c we take $b_{\min} = 10$, while for Mg – Mg at 4.5 A GeV/c and C – C at 4.2 A GeV/c, the parameter $b_{\min}$ is equal to 5.

3.1. Pion Cluster Distributions. The clusters are considered as four-dimensional objects and the same variables can be defined for them as for the particles.

Variables X_α^B and X_α^T for cluster α have the same meaning as for particle i (3—4).

$$X_\alpha^B = \frac{\hat{p}_\alpha \hat{p}_T}{\hat{p}_B \hat{p}_T} = \frac{M_\alpha \hat{V}_\alpha \hat{u}_T}{m_B \hat{u}_B \hat{u}_T}, \tag{14}$$

$$X_\alpha^T = \frac{\hat{p}_\alpha \hat{p}_B}{\hat{p}_B \hat{p}_T} = \frac{M_\alpha \hat{V}_\alpha \hat{u}_B}{m_T \hat{u}_B \hat{u}_T}, \tag{15}$$

where M_α is the effective mass of cluster α.

In Figures 3.1a, 3.1b and 3.1c we present the $XB - XT(X_\alpha^{beam} - X_\alpha^{target})$ plots for the pion clusters separated by using the algorithm described above.

For π^- – C, the beam and target fragmentation regions are clearly separated from one another. For nucleus-nucleus reactions the clusters cannot be found close to the axes, as in the case of single-particle plots. For Mg – Mg one can observe concentrations of points corresponding to the beam and target fragmentation regions; the separation is not distinct as for π^- – C. For C – C the fragmentation regions are more difficult to observe because the number of separated clusters is smaller.

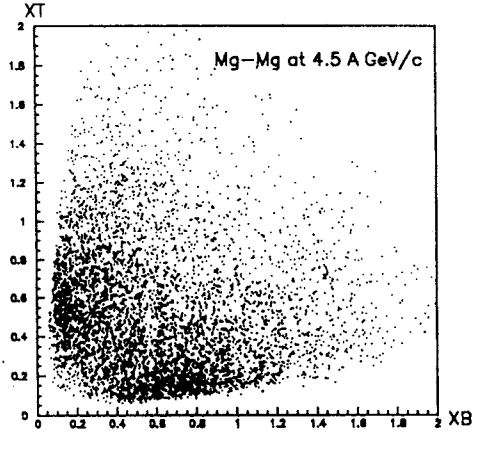

Fig.3.1a

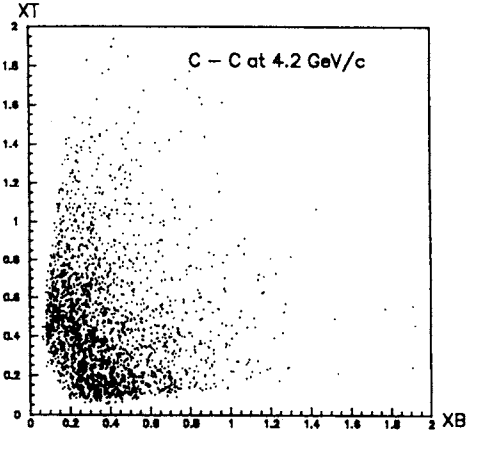

Fig.3.1b

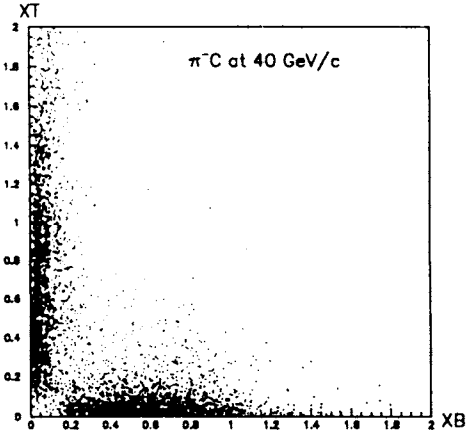

Fig.3.1c

Considering the distance from cluster to the primary particles, b_α^T and b_α^B, functions $F(b_\alpha^T)$ and $F(b_\alpha^B)$ can be determoned in the same way as for the single particles (7,8),

$$F(b_\alpha^T) = \frac{1}{\sigma}\int_\Omega \frac{2}{M_\alpha^2}\frac{1}{\sqrt{\frac{(b_\alpha^T)^2}{4}+b_\alpha^T}}\frac{d\sigma d\Omega_\alpha}{db_\alpha^T d\Omega_\alpha}, \tag{16}$$

$$F(b_\alpha^B) = \frac{1}{\sigma}\int_\Omega \frac{2}{M_\alpha^2}\frac{1}{\sqrt{\frac{(b_\alpha^B)^2}{4}+b_\alpha^B}}\frac{d\sigma d\Omega_\alpha}{db_\alpha^B d\Omega_\alpha}. \tag{17}$$

Tables 3.1a, 3.1b and 3.1c present the slopes for the pion clusters in the fragmentation regions of the target and the projectile.

The difference between the hadron-nucleus and nucleus-nucleus reactions is significant, as well as for single particles.

We also notice the difference between the nucleus-nucleus reactions Mg—Mg and C – C. As we mentioned before, for C – C less clusters can be separated, because of lower multiplicity. For Mg – Mg we have more particles in the final state as the streamer chamber makes it possible to select central collisions.

3.2. Asymptotic Properties of Pion Clusters. In [1—2] it was shown that the cluster width becomes constant ($\langle b_k \rangle = 4$) for large enough values of the energy $\sqrt{s}$; the asymptotic regime is reached for π^- – C at $p_{\text{beam}} = 40$ GeV/c.

Table 3.1a

Reaction	Fit parameters	Target fragm.	Beam fragm.
Mg — Mg at 4.5 GeV/c	A_1	0.34 ± 0.09	0.12 ± 0.08
	t_1	1.6 ± 0.1	1.7 ± 0.3
	A_2	0.71 ± 0.08	1.08 ± 0.07
	t_2	0.6 ± 0.1	0.72 ± 0.06

Table 3.1b

Reaction	Fit parameters	Target fragm.	Beam fragm.
C — C at 4.2 GeV/c	A_1	0.90 ± 0.05	0.88 ± 0.05
	t_1	1.05 ± 0.04	1.07 ± 0.03

Table 3.1c

Reaction	Fit parameters	Target fragm.	Beam fragm.
$\pi^- C$ at 40 GeV/c	A_1	1.00 ± 0.08	0.10 ± 0.01
	t_1	0.54 ± 0.05	11.1 ± 0.3
	A_2	0.23 ± 0.03	—
	t_2	2.0 ± 0.1	—

In Fig.3.2 we illustrate the dependence of the cluster width $\langle b_k \rangle$ on the energy $\sqrt{s}$ for different nuclear reactions.

As one can clearly see, the nucleus-nucleus reactions Mg—Mg and C—C at $p_{\text{beam}} \sim 4$ A GeV/c are localized in the pre-asymptotic region.

3.3. Comparison of Different Algorithms. In paper [3] we have described a new cluster finding algorithm:

The clusters are defined as groups of particles satisfying the following condition: for every pair in the group the distance between two particles b_{ik} is smaller than the given value b_0. For all the reactions we have used 4.

The main difference between this algorithm and the previous one lies in the possibility of getting any number of clusters. Besides, there are also particles which do not belong to any cluster. It would be interesting to compare the clusters created by means of different algorithms.

Tables 3.3a, 3.3b and 3.3c show the slopes of the invariant functions for the clusters separated with the help of these two different algorithms.

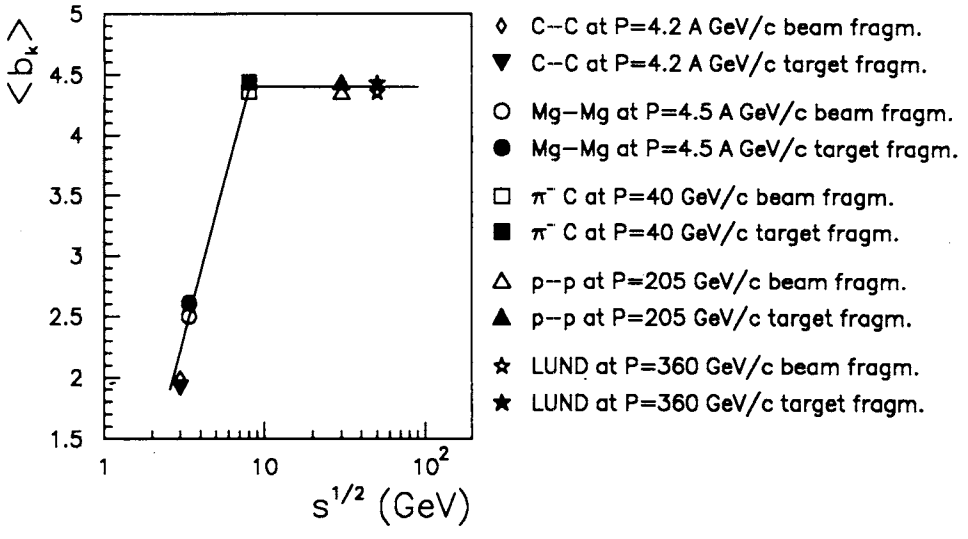

Fig.3.2

Table 3.3a

Mg — Mg at 4.5 GeV/c	Target	Target	Beam	Beam
	A_2^n	$b_{ik} \le b_0$	A_2^n	$b_{ik} \le b_0$
A_1	0.34 ± 0.09	0.77 ± 0.01	0.12 ± 0.08	0.34 ± 0.01
t_1	1.6 ± 0.1	1.32 ± 0.01	1.7 ± 0.3	2.57 ± 0.02
A_2	0.71 ± 0.08	—	1.08 ± 0.07	—
t_2	0.6 ± 0.1	—	0.72 ± 0.06	—

Table 3.3.b

C — C at 4.2 GeV/c	Target	Target	Beam	Beam
	A_2^n	$b_{ik} \le b_0$	A_2^n	$b_{ik} \le b_0$
A_1	0.90 ± 0.05	0.90 ± 0.02	0.88 ± 0.05	0.40 ± 0.01
t_1	1.05 ± 0.04	1.1 ± 0.01	1.07 ± 0.03	2.31 ± 0.03

For the $\pi^- - C$ reaction, the results do not significantly depend on the algorithm. For the nucleus-nucleus reactions the coefficients are close for the target fragmentation region, while they are different for the beam fragmentation region.

Table 3.3c

$\pi^- C$ at 40 GeV/c	Target	Target	Beam	Beam
	A_2^n	$b_{ik} \le b_0$	A_2^n	$b_{ik} \le b_0$
A_1	0.86 ± 0.11	1.3 ± 0.2	1.0	0.10 ± 0.01
t_1	0.69 ± 0.09	0.59 ± 0.07	10.0 ± 0.3	8.6 ± 0.5
A_2	0.14 ± 0.06	0.09 ± 0.03	—	—
t_2	2.20 ± 0.20	2.37 ± 0.03	—	—

4. Power Dependence of the $b_{\alpha\beta}$ Distribution

The relative invariant velocities b_{ik} can be used to describe any nuclear reaction. The experimental results have shown that the secondary particles are emitted mainly in the fragmentation regions of the primary particles, so, they can be separated into two independent groups (clusters), α and β. According to the automodelity and correlation depletion principles, the multiple production cross section can be expressed as follows [4]:

$$W(\ldots b_{ik} \ldots) = \frac{1}{b_{\alpha\beta}^m} W^{\alpha}\left(b_{\alpha i_\alpha}, \frac{b_{\alpha i_\beta}}{b_{\alpha\beta}}, \ldots\right) W^{\beta}\left(b_{\beta i_\beta}, \frac{b_{\beta i_\alpha}}{b_{\alpha\beta}}, \ldots\right), \tag{18}$$

where $b_{\alpha\beta}$ is the distance between the clusters (12).

As the distance between clusters is large enough ($b_{\alpha\beta} > 10$) this distribution is described by a power function:

$$\frac{1}{N}\frac{dN}{db_{\alpha\beta}} = \frac{A}{b_{\alpha\beta}^m}. \tag{19}$$

Table 4, shows the values of the m parameter obtained for various reactions and different algorithms to separate clusters.

It is very interesting that the parameter m has almost the same value for different reactions, irrespective of the algorithm used to separate the clusters.

Table 4

	$A_2^{\min}$	$b_{ik} \le b_0$
Mg — Mg at 4.5 GeV/c	3.6 ± 0.3	3.2 ± 0.1
C — C at 4.2 GeV/c	3.9 ± 0.1	3.5 ± 0.2
$\pi^- C$ at 40 GeV/c	3.0 ± 0.1	2.9 ± 0.2

5. Conclusions

A clear difference is seen between the hadron-nucleus and nucleus-nucleus reactions. It could be illustrated by discrepancy of plots $(X_i^B - X_i^T)$ and invariant functions $F(b_i^B)$, $F(b_i^T)$ for π measons. This difference becomes more significant for clusters. However we must stress the likeness of hadron-nucleus and nucleus-nucleus characteristics for power dependance for $b_{\alpha\beta}$ distribution (parameter m) for both algorithms.

The analysis of cluster and single-particle characteristics, plots $(X_\alpha^B - X_\alpha^T)$ and invariant functions $F(b_\alpha^B)$, $F(b_\alpha^T)$ shows:

For clusters, fragmentation regions are developed more weakly than for single-particle ones. More strong variation of slopes is observed for different reactions in the case of cluster distributions than for particles.

The invariant distributions of the clusters created by using different algorithms are almost the same for the hadron-nucleus but different for the nucleus-nucleus reactions (especially for the projectile fragmentation region).

6. Acknowledgments

We are pleased to thank Academician Baldin A.M. for fruitful discussions and permanent support in our work.

We also express our gratitude to the chamber division staff and, especially, to Dr.Kuznetsov A.A. for the opportunity to use their experimental material.

A similar contribution was reported to the XIII International Seminar on High Energy Physics Problems held in Dubna.

Our work was supported by the Russian Foundation for Fundamental Research.

References

1. Балдин А.М., Диденко Л.А. — Лекции для молодых ученых. В.43, ОИЯИ, Р1-87-912, Дубна, 1987.
2. Baldin A.M., Didenko L.A. — Forschtitte der Phys., 1990, v.38, No.4.
3. Gridnev T.G. et al. — JINR Preprint E1-93-98, Dubna, 1993.
4. Балдин А.М. — Препринт ОИЯИ Р2-94-463, Дубна, 1994.
5. Водопьянов А.С., Садовский А.Б. — Краткие Сообщения ОИЯИ, 1994, 5[68]-94, с.21.
6. Belaga V.V. et al. — JINR Preprint P1-95-233, Dubna, 1995.
7. Anikina M.H. et al. — JINR Rap. Comm., 1989, No.1[34]-89, p.8.
8. Балдин А.М. и др. — Ядерная физика. 1986, т.44, вып.5(11), с.1209.

Received on June 4, 1997.